

AD-A123 698

SIGNAL-TO-NOISE CONSIDERATIONS IN FLUCTUATION ANALYSIS

1/1

SPECTROSCOPIC TECH. (U) INDIANA UNIV AT BLOOMINGTON

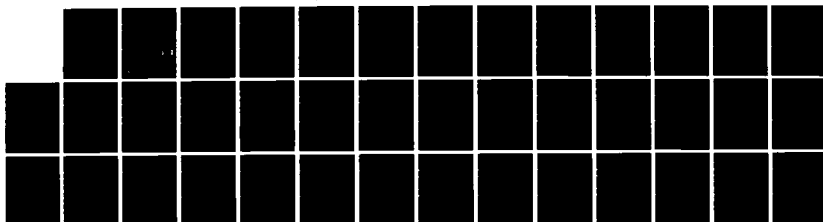
DEPT OF CHEMISTRY J M RAMSEY ET AL. 20 JAN 83

UNCLASSIFIED

INDU/DC/GMH/TR-83/52 N00014-76-C-0038

F/G 7/4

NL

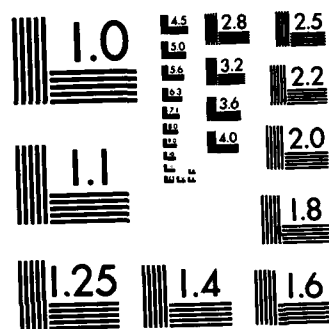


END

FILMED

X

DTIC



MICROCOPY RESOLUTION TEST CHART  
NATIONAL BUREAU OF STANDARDS-1963-A

UNCLASSIFIED

SECURITY CLASSIFICATION OF THIS PAGE (When Data Entered)

REPORT DOCUMENTATION PAGE		READ INSTRUCTIONS BEFORE COMPLETING FORM
1. REPORT NUMBER INDU/DC/GMH/TR-83-52	2. GOVT ACCESSION NO. AD-A123698	3. RECIPIENT'S CATALOG NUMBER 12
4. TITLE (and Subtitle) Signal-to-Noise Considerations in Fluctuation Analysis Spectroscopic Techniques (FAST)		5. TYPE OF REPORT & PERIOD COVERED Interim Technical Report
7. AUTHOR(s) J. M. Ramsey and G. M. Hieftje		6. PERFORMING ORG. REPORT NUMBER 61
9. PERFORMING ORGANIZATION NAME AND ADDRESS Department of Chemistry Indiana University Bloomington, IN 47405		8. CONTRACT OR GRANT NUMBER(s) N14-76-C-0838
11. CONTROLLING OFFICE NAME AND ADDRESS Office of Naval Research Washington, D.C.		10. PROGRAM ELEMENT, PROJECT, TASK AREA & WORK UNIT NUMBERS NR 051-622
14. MONITORING AGENCY NAME & ADDRESS (if different from Controlling Office)		12. REPORT DATE 20 January 1983
		13. NUMBER OF PAGES 34
		15. SECURITY CLASS. (of this report) UNCLASSIFIED
		15a. DECLASSIFICATION/DOWNGRADING SCHEDULE
16. DISTRIBUTION STATEMENT (of this Report) This document has been approved for public release and sale; its distribution is unlimited.		
17. DISTRIBUTION STATEMENT (of the abstract entered in Block 20, if different from Report)		
18. SUPPLEMENTARY NOTES Prepared for publication in ASTM PUBLICATION		
19. KEY WORDS (Continue on reverse side if necessary and identify by block number) time-resolved fluorescence frequency response signal-to-noise improvement instrumentation		
20. ABSTRACT (Continue on reverse side if necessary and identify by block number) It is possible to determine fluorescence lifetimes from the frequency response of a fluorophore as well as from its time response. Various schemes for measuring such a response curve are illustrated and include the use of sources whose intensity is modulated at single, swept frequencies, at several frequencies simultaneously, or over a broad, continuous band of frequencies. Detection methods which are considered include a single broad-frequency-response device, one which is swept, and another which hops from one modulated		

AD A 123698

DTIC FILE COPY

DTIC  
ELECTE  
JAN 24 1983  
S D

DD FORM 1473  
1 JAN 73EDITION OF 1 NOV 65 IS OBSOLETE  
S/N 0102-014-6601

UNCLASSIFIED

SECURITY CLASSIFICATION OF THIS PAGE (When Data Entered)

83

013

20. Abstract - continued

→ frequency to another. Signal-to-noise expressions are derived for each combination of source and detector and conclusions are drawn from comparison of the S/N expressions. From these considerations and the availability of existing sources for use in time-resolved fluorimetry, the most attractive approaches appear to be one which employs a source modulated at several frequencies simultaneously, each of which is monitored by its own tuned detector or a sinusoidally modulated source, swept synchronously with a tuned detector.

OFFICE OF NAVAL RESEARCH

Contract N14-76-C-0838

Task No. NR 051-622

SIGNAL-TO-NOISE CONSIDERATIONS IN FLUCTUATION  
ANALYSIS SPECTROSCOPIC TECHNIQUES (FAST)

by

J. M. Ramsey and G. M. Hieftje

Prepared for Publication

in

ASTM PUBLICATION

Indiana University  
Department of Chemistry  
Bloomington, Indiana 47405

20 January 1983

Accession For	
NTIS GRA&I	<input checked="checked" type="checkbox"/>
DTIC TAB	<input type="checkbox"/>
Unannounced	<input type="checkbox"/>
Justification	
By	
Distribution/	
Availability Codes	
Dist	Avail and/or Special
A	



Reproduction in whole or in part is permitted for  
any purpose of the United States Government

This document has been approved for public release  
and sale; its distribution is unlimited

## INTRODUCTION

A broad range of different chemical measurements involve a perturbation of the chemical system and the resulting measurement of the system's response to that perturbation [1-10]. For example, nuclear magnetic resonance (NMR) spectrometry is most commonly implemented by perturbing the nuclei to be examined with a pulse of radio-frequency energy and monitoring the response of the nuclei to that pulse; this response is termed the free-induction decay. Similarly, the kinetics of rapid chemical reactions are often investigated by perturbing the studied reaction with a pulse of electrical or thermal energy; monitoring the induced change in reaction equilibrium then permits the kinetics to be characterized. Finally, in gas chromatography, a pulse of a chemical sample is introduced into the instrument (a gas chromatograph) and the response of the instrument to that chemical "pulse" is the gas chromatogram itself.

The measurement of fluorescence lifetimes [1,4,6] and photochemical reaction rates [5] is often accomplished using this same impulse-based approach. Of the many techniques available for the determination of fluorescence lifetimes, the time-correlated single photon method [11-13] is now the most frequently used. Another common approach is phase/modulation fluorimetry [14,15]. This technique is a frequency-domain measurement and involves the determination of the systems frequency-response function. In these frequency-based techniques, the fluorophore or photolytic reaction to be studied is perturbed not with a pulse of light, but rather with a CW optical beam which is amplitude modulated. If the beam is modulated over a broad range of frequencies, either simultaneously or in a swept fashion, it is possible to monitor the frequency response of the fluorophore or reaction. Deducing the photolytic reaction rate or fluorescence lifetime using such a source is

possible either in the time domain, using correlation techniques [1,5,10] or in the frequency domain using spectrum analysis [16].

In the present paper, frequency-domain measurements will be reviewed and their application to the measurement of fluorescence lifetimes emphasized. Expressions will then be derived for the signal-to-noise ratios which should be possible with each of the alternative methods. Finally, the signal-to-noise expressions will be compared with a view toward identifying the optimal technique for obtaining fluorescence lifetimes. Throughout this discussion, the reader is encouraged to consider the application of these measurement principles to other areas, including the study of photolytic reactions, electrochemistry, radical-incuded reactions, etc.

#### FREQUENCY-BASED METHODS FOR LIFETIME DETERMINATION

The two alternative methods for the frequency-based measurement of fluorescence lifetimes or photolytic reaction rates are schematically illustrated in Fig. 1. The two cases employ a light source whose intensity is modulated, respectively, either stoichastically or sinusoidally. In Fig. 1, the determination of a fluorescence lifetime is used as an example; however, the general methodology would be the same no matter what the measurement might involve. Let us examine more closely these two techniques.

##### Swept-Frequency Method

Figure 1A portrays a swept-frequency approach to fluorescence lifetime determination. In this scheme an optical source (S) is used whose output intensity can be modulated at any desired frequency. This source illuminates

the sample cell (C) which contains the system whose response characteristics (fluorescence kinetics) are sought. The response of this system to the modulated source will be a time-varying fluorescence. Clearly, the intensity of the fluorescence will vary at the same frequency as the source because of the linear relationship between the two. This fluorescence is detected by a photomultiplier tube (PMT) and the resulting photocurrent is sent to an AC-to-DC converter. The AC-to-DC device puts out a DC signal which is proportional to the mean square amplitude (power) of the sinusoidal photocurrent signal. This signal can then be applied to the vertical axis of an X-Y recorder.

The optical source in Fig. 1A is driven by an oscillator which can sweep across the desired modulation frequencies. For convenience, a DC signal proportional to the frequency of modulation is sent to the X-axis of the X-Y recorder, so the recorder sketches the frequency response curve directly as the optical source modulation is swept across the desired frequencies. The assumptions made here are that the modulation depth of the source intensity is constant with frequency and that the frequency response of the detection system is flat over the range of interest. If these assumptions are not valid, a correction for the system's response will be required. Conveniently, the system response can be determined by inserting a scattering substance into the sample cell and sweeping once more the desired frequency range. Correction then requires a simple division of the total frequency response curve by that of the system above [16].

#### Wideband Modulation Method

A second approach to frequency-response determination is shown in Fig. 1B. In this case a wideband modulated source is utilized to perturb the



species in the sample cell (C). The term "wideband modulated" implies that the intensity fluctuations of this source contain many frequencies. These fluctuations might be coherent (pulsed) or incoherent (noise). This fluctuating source illuminates the sample cell and induces a fluorescence which is observed with a photomultiplier (PMT). The resultant photocurrent is then processed by a tuned electronic filter whose passband can be set at any desired frequency. That frequency passed by the tuned filter is processed by an AC-to-DC converter whose output feeds the Y-axis of an X-Y recorder. A signal from the filter which is proportional to its center frequency is applied to the X-axis of the X-Y recorder and the center frequency is scanned across the frequencies of interest. Consequently, the frequency response of the fluorescence system is traced out by the recorder. As in the previous (swept frequency) example, it has been assumed here that the power spectrum of the intensity fluctuations from the source and the detector response are both constant with frequency. Of course, if this latter condition is not met, it is simple to correct for any of these changes through use of the same normalization procedures discussed earlier.

There are many possible variations to both of these schemes. In the first method (Fig. 1A), a tuned filter could be placed between the PMT and the AC-to-DC converter to reduce the noise which is detected. For the second scheme (Fig. 1B), the source could be modulated at all frequencies simultaneously or at only a number of discrete frequencies. Additionally, the detection system could be multiplexed rather than scanned. That is, a detection system could be employed that examines all frequencies simultaneously. Such a system might be a continuous digitizer followed by numerical

Fourier transformation or a number of detectors and tuned filters each of which observes a given frequency continuously. The advantages or disadvantages of all these schemes can best be decided through a signal-to-noise analysis.

### SIGNAL-TO-NOISE COMPARISON OF METHODS

#### FOR FREQUENCY-RESPONSE DETERMINATION

In the following analysis, it will be assumed that all measurements are limited in precision by photon shot noise. That is, the dominant noise in the measurement system will be assumed to be that caused by the inherent quantum fluctuations in a detected optical signal. Any optical measurement can theoretically be improved to this limiting situation.

The power spectrum for a shot-noise-limited process can be expressed by Eq. 1 [17].

$$S(\omega) = \phi \hat{S}(\omega) + \phi^2 \delta(\omega) \quad (1)$$

In Eq. (1),  $\phi$  is the average photon flux,  $\omega$  is angular frequency,  $\hat{S}(\omega)$  is the power spectrum of a single event in the process (i.e., here the arrival of a photon), and  $\delta$  is the Dirac delta function. Because the arrival of a photon is essentially an instantaneous event (i.e., a delta function in time),  $\hat{S}(\omega)$  can be set to a constant of magnitude one. In this discussion it will be assumed that the photon flux (radiant power) is directly proportional to the observed photocurrent, i.e., quantum and collection efficiencies will be neglected. In such a situation the power spectrum of the induced photocurrent for an optical flux  $\phi$  will consist of a DC electrical power (not

current) of  $\phi^2$  and a power of  $\phi$  at all other frequencies. The power at frequencies greater than zero is due to the fluctuations inherent in the shot-noise process. Notice that the AC power or noise power per unit bandwidth is just the square root of the DC power. One should also note that throughout the following discussion the term "power" refers to the electrical power generated by the photon detection process.

#### Swept-Frequency Method

In the swept-frequency method the perturbation consists of a modulated photon flux. The time-dependent input to the system  $[i(t)]$  can thus be described as a 100% modulated sinusoid at any frequency  $\omega_0$ , viz.,

$$i(t) = \phi[1 + \cos(\omega_0 t + \phi)] \quad . \quad (2)$$

The positive-frequency Fourier transform of  $i(t)$  is

$$I(\omega) = \phi[\delta(\omega) + \delta(\omega - \omega_0)] \quad . \quad (3)$$

The signal power spectrum,  $S(\omega)$ , is then

$$S(\omega) = \phi^2[\delta(\omega) + \frac{1}{2} \delta(\omega - \omega_0)] \quad . \quad (4)$$

In addition, if one assumes Poisson statistics for the arrival of photons, the noise power per unit bandwidth,  $N(\omega)$ , for the input signal,  $i(t)$ , is

$$N(\omega) = \phi \quad . \quad (5)$$

The total power spectrum (noise plus signal) for this case is illustrated in Fig. 2. In Fig. 2, the shot-noise contribution is the constant (with frequency) power level of magnitude  $\phi$ . There is also a signal contribution to Fig. 2, visible as both a DC term and as an AC term at frequency  $\omega_0$ . Both of these signals stand above the level of background noise by an amount  $\phi^2$  and  $\phi^2/2$  for the DC and AC terms, respectively; thus their respective peak magnitudes will be  $\phi^2 + \phi$  and  $(\phi^2/2) + \phi$ . Of these components, it is the signal-to-noise ratio for the measurement of the AC power at  $\omega_0$  that is of interest here. The signal-to-noise ratio (S/N) is defined to be the mean signal divided by the square root of the variance of that signal [18], viz.,

$$\frac{S}{N} = \frac{\text{mean signal}}{(\text{variance of signal})^{1/2}} \quad (6)$$

The mean signal in this case is known to be  $\phi^2/2$ , the power at  $\omega_0$ . The noise in the measurement will be entirely due to the shot-noise power at frequencies near  $\omega_0$ . A power spectrum analyzer (the device used to measure power spectra) records the mean-square signal,  $\psi^2$ , over some bandwidth  $B_e$ , indicated on Fig. 2. The variance of the mean square value in the case of spectrally flat noise across a given bandwidth  $B_e$  is given by Eq. (7) [19].

$$\text{Var} [\psi^2] = \frac{C_N^2(0)}{B_e \tau} + \frac{2\mu_N^2}{B_e \tau} C_N(0) \quad (7)$$

In Eq. (7),  $C_N(0)$  is the value of the autocovariance function at zero delay of the noise contained in the bandwidth  $B_e$ ,  $\mu_N$  is the mean value of the noise, and  $\tau$  is the time over which the measurement is averaged. The auto-

covariance is the autocorrelation minus the square of the mean [20]. Because only AC components are being observed over bandwidth  $B_e$ , the second term of Eq. (7) will be zero. The factor  $C_N(0)$  is equal to the mean square noise observed in the measurement, in this case  $B_e \phi$ . Eq. (7) now becomes

$$\text{Var} [\phi^2] = \frac{B_e \phi^2}{\tau} \quad (8)$$

The known mean and variance of the signal can be substituted into Eq. (6) to yield

$$\frac{S}{N} = \frac{\phi}{2} \left( \frac{\tau}{B_e} \right)^{1/2} \quad (9)$$

Eq. (9) implies that S/N will increase proportionally with power, the square root of the averaging period, or the reciprocal of the square root of the measurement bandwidth. This result indicates that a large increase in S/N could be realized if a tuned filter, whose center frequency follows the source modulation frequency, were placed between the PMT and the AC-to-DC converter shown in Fig. 1A. Specifically, if the entire bandwidth over which measurements are to be made is  $B_w$  and the bandwidth of the tuned filter is  $B_e$ , the S/N gain would be  $(B_w/B_e)^{1/2}$ .

Figure 2 indicates that background subtraction would also be needed to find the AC power. This second measurement would increase the variance of the procedure by a factor of two, and thereby decrease S/N by a factor of  $(2)^{1/2}$ . For brevity of expression, this factor will be neglected in all subsequent treatment; it would be present in all the S/N expressions discussed later so nothing is lost when they are compared. In addition, the exact

signal-to-noise expressions should be frequency-dependent functions. The signal measured will decrease with increasing frequency according to the systems frequency-response function. If we assume constant fluorescence quantum efficiency, changes in lifetime will only effect the signal factor in the expressions and not the noise component. Thus, multiplication of equation (9) by the system frequency-response function would make it valid for all frequency measurements. Because we are comparing the relative signal-to-noise ratio of several different measurement schemes, this frequency dependent factor becomes irrelevant and is not included in the following equations.

### Wideband Modulation Method

For the second measurement scheme, shown in Fig. 1B, there can be two cases of interest: a multi-frequency intensity-modulated source and a broadband intensity-modulated source. The latter is the continuous case of the former. Let us consider separately the S/N available from each approach.

Multi-frequency Modulation. The time-dependent intensity,  $i(t)$ , from a multi-frequency modulated source can be expressed by Eq. (10). This source is assumed to be simultaneously amplitude modulated at  $K$  discrete frequencies. This situation simulates the behavior of mode noise in a CW laser [8,10,16].

$$i(t) = \sum_{n=1}^K \phi_n [1 + \cos(\omega_n t + \phi_n)] \quad (10)$$

where  $\phi_n$  is the amplitude of the  $n^{\text{th}}$  modulation frequency ( $\omega_n$ ) and  $\phi_n$  the phase of the  $n^{\text{th}}$  frequency component. The Fourier transform of this signal is

$$I(\omega) = \sum_{n=1}^K \phi_n \delta(\omega) + \sum_{n=1}^K \phi_n \delta(\omega - \omega_n) e^{i\phi_n} \quad (11)$$

For the situation where all  $\phi_n$  are the same in magnitude and equal to  $\phi$ , the power spectrum of  $i(t)$  is

$$S(\omega) = K^2 \phi^2 \delta(\omega) + \sum_{n=1}^K \frac{\phi^2}{2} \delta(\omega - \omega_n) \quad (12)$$

As expressed in Eq. (5), the noise power per unit bandwidth,  $N(\omega)$ , is the

square root of the DC (left-hand) term of  $S(\omega)$ , or  $N(\omega) = K\phi$ . The variance produced by the shot noise will be, in this case,

$$\text{Var}[\Psi^2] = \frac{E}{\tau} (K\phi)^2 \quad (13)$$

The S/N will then be

$$\frac{S}{N} = \left( \frac{\tau}{B_e} \right)^{1/2} \frac{\phi}{2K} \quad (14)$$

Comparing the S/N for the multi-frequency modulated method [Eq.(14)] to that for the swept-frequency system [Eq. (9)], one finds that the S/N is worse in the former case by a factor of  $K$ , when equal bandwidths ( $B_e$ ) are employed in both methods. This situation arises because the power of the average detected quantity has increased by a factor of  $K^2$  in the multi-frequency technique, but the power at each modulation frequency has remained the same. Thus the noise level has increased by  $K$ , whereas no increase in the measured signal is realized.

Broadband Modulation. The second case of interest for the Fig. 1B measurement scheme occurs when broadband modulation is employed. In this case, modulation arises simultaneously at every frequency across the entire band of interest. An expression for the time-dependent signal for this case can be obtained if one takes the limit in Eq. (10) as  $K \rightarrow \infty$  and  $\omega_0 \rightarrow 0$  while  $\omega_0 K$  is kept constant and equal to the entire frequency range of interest ( $B_w$ ). The required operation is expressed in Eq. (15).



$$i(t) = \lim_{\substack{K \rightarrow \infty \\ \omega_0 \rightarrow 0 \\ \omega_0 K = B_w}} \sum_{n=1}^K \phi_n [1 + \cos(n\omega_0 t + \phi_n)] \quad (15)$$

At these limits, the summation becomes an integral:

$$i(t) = \int_0^{B_w} \phi(\omega) [1 + \cos(\omega t + \phi(\omega))] d\omega \quad (16)$$

Once more if the modulation amplitude  $[\phi(\omega)]$  is constant and equal to  $\phi$ ,  $i(t)$  becomes

$$i(t) = \phi B_w + \phi \int_0^{B_w} \cos[\omega t + \phi(\omega)] d\omega \quad (17)$$

The Fourier transform of Eq. (17) is then

$$I(\omega) = \int_{-\infty}^{\infty} e^{-j\omega t} \left\{ \phi B_w + \phi \int_0^{B_w} \cos[\omega' t + \phi(\omega')] d\omega' \right\} dt \quad (18)$$

where the primes have been included to distinguish the separate frequency variables. The first term in Eq. (18) is the DC term which is straightforward to evaluate. The second term is most easily evaluated by expansion of the cosine into its complex exponential form and interchange of the order of integration. Performing these operations yields

$$I(\omega) = \phi B_w \delta(\omega) + \phi \int_0^{B_w} e^{j\phi(\omega')} \delta(\omega - \omega') d\omega' \quad (19)$$

Integrating over  $\omega'$  now gives

$$I(\omega) = \phi B_w \delta(\omega) + \phi e^{j\phi(\omega)} \quad \text{for } 0 \leq \omega \leq B_w . \quad (20)$$

The power spectrum for  $i(t)$  in this case is then

$$S(\omega) = \phi^2 B_w^2 \delta(\omega) + \frac{\phi^2}{2} \quad \text{for } 0 \leq \omega \leq B_w . \quad (21)$$

Eq. (21) indicates that a component in the signal power spectrum exists at DC (left-hand term) which is  $2B_w^2$  larger than the components at other frequencies. However, the power spectrum at frequencies above zero has a constant magnitude out to frequency  $B_w$ . As mentioned earlier, this sort of spectrum is commonly called a flat or "white" spectrum.

The noise for the case pertaining to Eq. (21) is, as in the previous two analyses, the square root of the DC term. The noise per unit bandwidth is then

$$N(\omega) = \phi B_w . \quad (22)$$

The variance of the measurement in this case using Eq. (7) is

$$\text{Var}[\Psi^2] = \frac{B_e B_w^2 \phi^2}{\tau} \quad (23)$$

where all quantities are as defined earlier. Because the signal is continuously spread over frequency space, the observed signal power is directly proportional to the bandwidth of the detection system. Therefore, the S/N expression for this case is

$$\frac{S}{N} = \frac{\phi}{2B_w} (\tau B_e)^{1/2} \quad (24)$$

For comparison to the previous two S/N expressions, Eq. (24) can be rewritten as

$$\frac{S}{N} = \frac{\phi B_e}{2B_w} \left( \frac{\tau}{B_e} \right)^{1/2} \quad (25)$$

Comparison of Eqs. (9) and (25) shows that the S/N for broadband modulation will be reduced by a factor of  $B_e/B_w$  over that of the swept-frequency method, even though the average total power of the signal is  $B_w^2$  greater. To better compare the S/N for the three methods discussed above and expressed by Eqs. (9), (14), and (25), each of the quantities  $B_e$ ,  $B_w$ , and  $\phi$  will be set equal in all expressions. It will also be assumed that each measurement is carried out with the swept-detection filter approach, so  $\tau$  will be the same in all situations. Typical values for  $B_w$ ,  $B_e$ , and  $K$  would be  $10^9$  Hz,  $10^5$  Hz and 40, respectively, for experiments aimed at determining luminescence lifetimes [10,16]. For these conditions the multi-frequency modulation scheme would have S/N a factor of 40 smaller and the broadband modulation method a factor of  $10^4$  smaller than the swept-frequency method.

Of course, the broadband modulation methods lend themselves to multiplex signal processing and would benefit from such a scheme. Multiplex processing involves modifying the signal observation time ( $\tau$ ) in the above expressions. Such a technique is considered next.

#### Alternative Schemes for Data Acquisition

Schemes for data acquisition such as multiplex and slew-scan [21] can be compared in terms of the time spent monitoring each spectral resolution element,  $\tau$ , expressed in turn as a function of the total time required to perform an

experiment,  $T$ . The total experiment time  $T$  will be assumed constant for all comparisons discussed in this section.

Swept-Frequency Method. The time per resolution element,  $\tau$ , for this method will be simply the total time,  $T$ , divided by the number of resolution elements,  $M$ . In turn,  $M$  will be the total bandwidth of the experiment,  $B_w$ , divided by the bandwidth of the detection system,  $B_e$ :

$$M = \frac{B_w}{B_e} \quad (26)$$

The time per resolution element is therefore

$$\tau = \frac{TB_e}{B_w} \quad (27)$$

This expression can then be substituted into Eq. (9).

Multi-frequency Modulation. For this scheme, there are three possible detection modes: continuous sweep, slew-scan, and multiplex. The continuous-sweep case is similar to the swept frequency method discussed above. In contrast, slew-scan operation involves stepping instantaneously between modulation frequencies and observing every one for an equal amount of time. Finally, multiplex detection requires simultaneous detection of all modulation frequencies, using a number of detectors equal to the number of those frequencies. As a consequence, each detector observes the signal for the entire observation time,  $T$ . The expressions for  $\tau$  for each of these cases follow.

Case 1: continuous sweep detection

This expression is identical to that derived for the swept-frequency method, i.e., the total time divided by the number of resolution elements:

$$\tau = \frac{TB_e}{B_w} \quad (28)$$

Case 2: slew-scan detection

If the transition between modulation frequencies is instantaneous, the measurement time will be equally divided among the K discrete frequencies, so

$$\tau = \frac{T}{K} \quad (29)$$

Case 3: multiplex detection

When each of k detectors observes a single modulation frequency,

$$\tau = T \quad (30)$$

All of these expressions can be substituted into Eq. (14) to compare S/N ratios.

Broadband Modulation. This scheme can be carried out using only two of the possible signal acquisition methods:

Case 1: continuous sweep

As with the swept-frequency and multi-frequency modulation methods,

$$\tau = \frac{TB_e}{B_w} \quad (31)$$

Case 2: multiplex

The most extensive multiplex approach involves a single detector for each spectral resolution element contained in the bandwidth of interest,

i.e.,  $B_w/B_e$  detectors. Each detector would observe a given band of frequencies for the total time:

$$\tau = T \quad . \quad (32)$$

Alternatively, digitization of the signal from a single detector could be performed and be followed by Fourier transformation. Complying with signal recovery requirements, this latter approach would also yield  $B_w/B_e$  spectral resolution elements and Eq. (32) would apply for each element.

The expressions for case 1 and case 2 above can be substituted into Eq. (25) for a S/N comparison.

#### Summary of Expressions for Signal-to-Noise Ratio

Table I collects all the expressions for S/N derived above; all expressions are written in terms of the total experiment time, T. For purposes of comparison, each expression in Table I has been normalized by the swept-frequency expression and listed in Table II.

The first column in Table II, representing the continuous sweep scheme, indicates that S/N will be reduced by  $K^{-1}$  and  $B_e/B_w$ , respectively, for the multifrequency and broad-band modulation approaches compared to single-frequency modulation. The S/N for the multi-frequency approach could be improved by the slew-scan detection scheme as long as  $B_e K$  is less than  $B_w$ . The multiplex scheme shows further improvements in S/N for both the multi-frequency and broadband modulation methods. From these considerations, the multi-frequency modulation approach, coupled with multiplex detection, should provide the greatest signal-to-noise ratios for response evaluation. Next most efficient would be either the single frequency input with swept-bandpass detection or the multi-frequency input coupled with slew-scan detection, depending on the relative magnitudes of the parameters in Table II.

Table III lists relative values obtained from the expressions of Table II for the conditions specified earlier, i.e.,  $B_w = 10^9$  Hz,  $B_e = 10^5$  Hz, and  $K = 40$ . Clearly, the broadband modulation approach suffers severely in the S/N comparison. The multiple-frequency modulation approach also suffers unless one of the more sophisticated detection schemes is utilized.

Signal-to-Noise Ratios for Identical Input DC Radiant Power

It should be recalled that the average signal power is  $K^2$  and  $B_w^2$  greater for the multi-frequency and broadband modulation approaches, respectively, than for single frequency modulation. This situation is not realistic in most experimental situations. In many instances the optical power used to illuminate a system under study is limited to some upper level because of photodestruction or non-linearity of the system or by the capability of the optical source itself. Accordingly, it is useful to express S/N in Tables I and II in terms of equal average signal levels.

As before, the swept-frequency modulation method is chosen as the standard for comparison, and the other methods will be normalized to the same DC power. The average power input in that scheme was  $\phi^2$ , yielding

$$\frac{S}{N} = \frac{\phi}{2} \left( \frac{\tau}{B_e} \right)^{1/2} \quad (33)$$

Multi-frequency Modulation. In the multi-frequency modulation method, the average (DC) power was assumed to be  $K^2\phi^2$  for  $K$  modulation frequencies [cf. Eq. (12)]. The power at each modulation frequency would then have to be  $\phi^2/K^2$  to reduce this DC term to  $\phi^2$ , the same magnitude as the DC term in

the single swept-frequency modulation scheme. The expression for the power spectrum,  $S(\omega)$ , for this situation would then become

$$S(\omega) = \phi^2 \delta(\omega) + \sum_{n=1}^K \frac{\phi^2}{2K^2} \delta(\omega - \omega_n) \quad (34)$$

Writing  $S/N$  as in Eq. (14) yields

$$\frac{S}{N} = \frac{\phi}{2K^2} \left( \frac{\tau}{B_e} \right)^{1/2} \quad (35)$$

The noise has been reduced by a factor of  $K$  because of the decreased DC term but the signal has been reduced by  $K^2$ ; hence Eq. (35) is a factor of  $K$  smaller than the previous result in Eq. (14).

Broadband Modulation. As indicated by Eq. (21), the power per unit bandwidth at positive frequencies will have to be reduced to  $\phi^2/2B_w^2$  to reduce the DC term to  $\phi^2$ . With the DC power reduced to  $\phi^2$ , the power spectrum expression,  $S(\omega)$ , for this method becomes

$$S(\omega) = \phi^2 \delta(\omega) + \frac{\phi^2}{2B_w^2} \quad (0 \leq \omega \leq B_w) \quad (36)$$

and produces

$$\frac{S}{N} = \frac{\phi B_e}{2B_w^2} \left( \frac{\tau}{B_e} \right)^{1/2} \quad (37)$$

Similar to the multi-frequency modulation method, the noise here has been



reduced by  $B_w$  but the signal has been reduced by  $B_w^2$ , making S/N lower by a factor of  $B_w$  over Eq. (35).

#### Summary of Signal-to-Noise Expressions for Identical DC Power

Table IV summarizes the S/N expressions in Eqs. (33), (35), and (37). These expressions, when normalized by the swept single-frequency case, are listed in Table V. Table V shows that there is an additional  $K^{-1}$  term in all the expressions for multi-frequency modulation and an additional  $B_w^{-1}$  term in the expressions for broadband modulation compared with those in Table II.

Inspection of Table V shows that the multi-frequency modulation approach, coupled with either slew-scan or multiplex detection, could potentially provide the greatest signal-to-noise ratios. Swept single-frequency modulation would be the next most efficient measurement method. The actual ranking of these techniques in terms of the highest S/N depends, of course, upon the values of  $B_w$ ,  $B_e$ , and  $K$ , as shown in Table VI.

Table VI mimics Table V where the expressions have been evaluated for the conditions,  $B_w = 10^9$  Hz,  $B_e = 10^5$  Hz, and  $K = 40$ . These results show that under the condition of identical DC power the single swept-frequency approach is by far the best.

#### CONCLUSIONS

From Tables V and VI, it would seem that realistic laboratory-based measurements could best be made using a swept-frequency amplitude-modulated source and a frequency-selective detector whose bandpass tracks the modulation frequency. To determine brief fluorescence lifetimes from a fre-

quency-response plot requires the use of high modulation frequencies [22,23]. For example, to generate a substantial portion of the frequency response spectrum of a fluorophore having a lifetime of 1 ns would require modulation frequencies as great as 1 GHz. Sources modulated at such high frequencies are not commonplace. A source that might be suitable for swept modulation frequency measurements is a laser/Bragg cell combination [24]. Modulation frequencies greater than 1 GHz have been obtained with this type of source. Swept modulation frequency systems in the 1-100 MHz range can be constructed using Pockels cell modulators [25]. Discrete modulation frequencies from 400-1000 MHz can also be obtained from a CW ion laser when operated under the proper conditions [26].

From a signal-to-noise standpoint, the next most attractive technique would involve the use of a source which is simultaneously modulated at a number of discrete frequencies, each of which is monitored continuously. Such a scheme is already feasible, although it has not yet been reported in the literature. As suggested earlier, a CW laser is such a multi-frequency source [10,16] and is simultaneously modulated at a large number of frequencies by the beating of its longitudinal modes with each other. This source does not exactly fit the model of a multifrequency modulated source used in this study in that the DC component of the intensity can be considerably larger than predicted here. The larger DC component will reduce the signal-to-noise ratio for a frequency response measurement but does not reduce the relative advantages of using multiplex detection. To detect each of the mode beat frequencies individually would require a number of tuned radio-frequency filters; conveniently, such filter technology is highly developed and forms a strong component of radio and television electronics. One would envision such a detection scheme to be relatively simple to construct and to operate. The design of such a device is now under-

The only scheme outlined in Tables V and VI which has been experimentally studied is the multi-frequency modulated source coupled with a swept-frequency detector [16]. Based on the success of those preliminary studies, and the expected gain in S/N of 100 afforded by multiplex detection, one would surmise the frequency-response approach to time-resolved fluorimetry to be a viable one.

## ACKNOWLEDGEMENT

Supported in part by the Office of Naval Research and by the National Science Foundation.

REFERENCES

1. Ramsey, J. M., Hieftje, G. M., and Haugen, G. R., Appl. Optics **18**, 1913 (1979).
2. Ramsey, J. M., Hieftje, G. M., and Haugen, G. R., Rev. Sci. Instrum. **50**, 997 (1979).
3. Hieftje, G. M. and Horlick, G., American Laboratory **13**, 76 (1981).
4. Hieftje, G. M. and Haugen, G. R., Anal. Chem. **53**, 755A (1981).
5. Haugen, G. R., Hieftje, G. M., Steinmetz, L. L., and Russo, R. E., Appl. Spectrosc. **36**, 203 (1982).
6. Russo, R. E. and Hieftje, G. M., Appl. Spectrosc. **36**, 92 (1982).
7. Horlick, G. and Hieftje, G. M. in Topics in Analytical and Clinical Chemistry, Vol. 3, D. M. Hercules, G. M. Hieftje, L. R. Snyder, and M. A. Evenson, Eds., Plenum Press, New York, 1978, Chapter 4, pp. 153-216.
8. Hieftje, G. M., Ramsey, J. M., and Haugen, G. R., in New Applications of Lasers to Chemistry, ACS Symposium Series no. 85, G. M. Hieftje, Ed., American Chemical Society, Washington, D.C., 1978, Chapter 8, pp. 118-125.
9. Hieftje, G. M. and Vogelstein, E. E., in Modern Fluorescence Spectroscopy, Vol. 4, E. Wehry, Ed., Plenum Press, New York, 1981, Chapter 2, pp. 25-50.
10. Dorsey, C. C., Pelletier, J. M., and Harris, J. M., Rev. Sci. Instrum. **50**, 333 (1979).
11. Knight, A. E. W. and Selinger, B. K., Austr. J. Chem. **26**, 1 (1973).
12. Lewis, C. and Ware, W. R., Rev. Sci. Instrum. **44**, 107 (1973).
13. Cline-Love, L. J. and Shaver, L. A., Anal. Chem. **48**, 364A (1976).
14. Gaviola, E., Z. Physik **35**, 748 (1926).
15. Birks, J. B. and Munro, I. H., in Progress in Reaction Kinetics, Vol. 4, G. Porter, Ed., Pergamon Press, New York, 1967, Chapter 7, pp. 239-303.

16. Hieftje, G. M., Haugen, G. R., and Ramsey, J. M., *Appl. Phys. Lett.* 30, 463 (1977).
17. Davenport, W. B., Jr. and Root, W. L., Random Signals and Noise, McGraw-Hill, New York, 1958.
18. Hieftje, G. M., *Anal. Chem.* 44 (6), 81A (1972).
19. Bendat, J. S. and Piersol, A. G., Random Data: Analysis and Measurement Procedures, Wiley-Interscience, New York, 1971.
20. Bracewell, R. N., The Fourier Transform and Its Application, 2nd ed., McGraw-Hill, New York, 1978.
21. Winefordner, J. D., Avni, R., Chester, T.L., Fitzgerald, J.J., Hart, L. P., Johnson, D. J., and Plankey, F. W., *Spectrochim. Acta* 31B, 1 (1976).
22. Spencer, R. D. and Weber, G., *Ann. N.Y. Acad. Sci.* 158, 361 (1969).
23. Harr, H. P. and Hanser, M., *Rev. Sci. Instrum.* 49, 632 (1978).
24. Lytle, F. E. Pelletier, M. J., and Harris, T. D., *Appl. Spectrosc.* 33, 28 (1979).
25. Hauser, M. and Heidt, G., *Rev. Sci. Instrum.* 46, 470 (1975).
26. Ramsey, J. M., *J. Appl. Phys.* 53, 1381 (1982).

TABLE I. Expressions for Signal-to-Noise Ratio for Various Frequency-Response Determination Approaches.<sup>a</sup>

Detection Method  Input Mode			
	swept frequency	slew scan	multiplex
single frequency modulation	$\frac{\phi}{2} \left( \frac{T}{B_w} \right)^{1/2}$	—	—
multi-frequency modulation	$\frac{\phi}{2K} \left( \frac{T}{B_w} \right)^{1/2}$	$\frac{\phi}{2K} \left( \frac{T}{B_e K} \right)^{1/2}$	$\frac{\phi}{2K} \left( \frac{T}{B_e} \right)^{1/2}$
broadband modulation	$\frac{\phi B_e}{2B_w} \left( \frac{T}{B_w} \right)^{1/2}$	—	$\frac{\phi}{2B_w} (TB_e)^{1/2}$

- <sup>a</sup>  $\phi$  is the photon flux,  $T$  is the total time taken to perform an experiment,  $K$  is the number of modulation frequencies,  $B_w$  is the total bandwidth over which the experiment is performed, and  $B_e$  is the detection system bandwidth.

TABLE II. Expressions for Signal-to-Noise Ratio from Table I  
Normalized by the Swept-Frequency Expression.<sup>a</sup>

Detection Method  Input Mode			
	swept frequency	slew scan	multiplex
single frequency modulation	1	—	—
multi-frequency modulation	$1/K$	$\frac{1}{K} \left( \frac{B_w}{B_e K} \right)^{1/2}$	$\frac{1}{K} \left( \frac{B_w}{B_e} \right)^{1/2}$
broadband modulation	$\frac{B_e}{B_w}$	—	$\left( \frac{B_e}{B_w} \right)^{1/2}$

<sup>a</sup> K is the number of modulation frequencies,  $B_w$  is the total bandwidth over which the experiment is performed and,  $B_e$  is the bandwidth of the detection system.



TABLE III. Signal-to-Noise Ratio Expressions from Table I  
 Normalized by the Single Swept-frequency Expression and  
 Evaluated for the Conditions,  $B_w = 10^9 \text{ Hz}$ ,  $B_e = 10^5 \text{ Hz}$ ,  
 $K = 40$ .<sup>a</sup>

Input Mode	Detection Method		
	swept frequency	slew scan	multiplex
single frequency modulation	1	—	—
multi-frequency modulation	0.025	0.395	2.5
broadband modulation	$10^{-4}$	—	$10^{-2}$

<sup>a</sup>  $B$  is the total bandwidth over which the experiment is performed,  
 $B_w$  is the detection system bandwidth, and  $K$  is the number of modulation  
 frequencies for multi-frequency modulation.

TABLE IV. Expressions for Signal-to-Noise Ratio Under Conditions of Identical Input DC Radiant Power.<sup>a</sup>

Input Mode \ Detection Method			
	swept frequency	slew scan	multiplex
single frequency modulation	$\frac{\phi}{2} \left( \frac{T}{B_w} \right)^{1/2}$	—	—
multi-frequency modulation	$\frac{\phi}{2K^2} \left( \frac{T}{B_w} \right)^{1/2}$	$\frac{\phi}{2K^2} \left( \frac{T}{KB_c} \right)^{1/2}$	$\frac{\phi}{2K^2} \left( \frac{T}{B_e} \right)^{1/2}$
broadband modulation	$\frac{\phi B_e}{2B_w^2} \left( \frac{T}{B_w} \right)^{1/2}$	—	$\frac{\phi}{2B_w^2} (TB_c)^{1/2}$

<sup>a</sup>  $\phi$  is the photon flux, T is the total time taken to perform an experiment, K is the number of modulation frequencies,  $B_w$  is the total bandwidth over which the experiment is performed, and  $B_e$  is the detection system bandwidth.

TABLE V. Signal-to-Noise Ratio Expressions From Table IV  
Normalized by the Swept-Frequency Expression.<sup>a</sup>

Input Mode	Detection Method	slew frequency	slew scan	multiplex
single frequency modulation		1	—	—
multi-frequency modulation		$\frac{1}{K^2}$	$\frac{1}{K^2} \left( \frac{B_w}{KB_e} \right)^{1/2}$	$\frac{1}{K^2} \left( \frac{B_w}{B_e} \right)^{1/2}$
broadband modulation		$\frac{B_e}{B_w^2}$	—	$\frac{1}{B_w} \left( \frac{B_e}{B_w} \right)^{1/2}$

<sup>a</sup> K is the number of modulation frequencies,  $B_w$  is the total bandwidth over which the experiment is performed, and  $B_e$  is the bandwidth of the detection system.

TABLE VI. Signal-to-Noise Ratio Expressions From Table IV  
 Normalized by the Single Swept-Frequency Expression and  
 Evaluated for the Conditions,  $B_w = 10^9 \text{ Hz}$ ,  $B_e = 10^5 \text{ Hz}$ ,  
 and  $K = 40$ .<sup>a</sup>

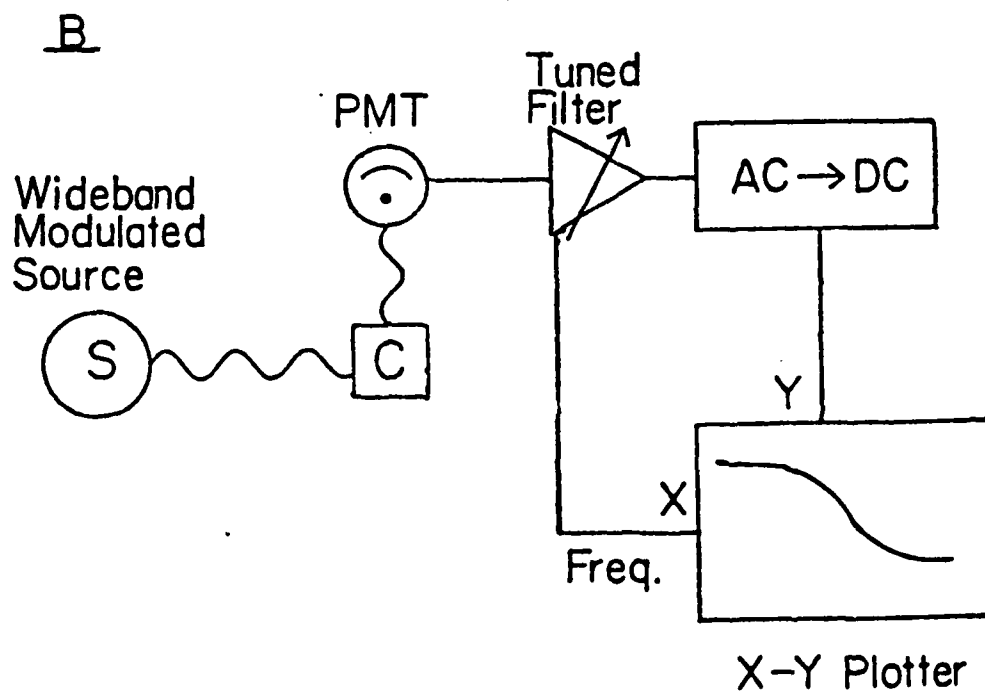
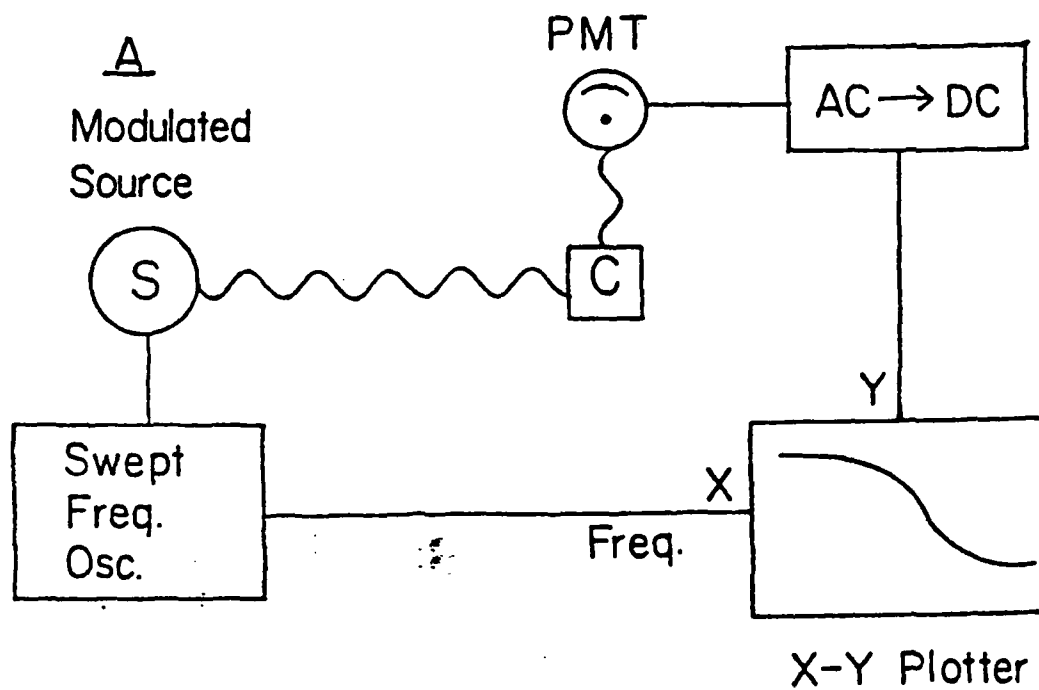
Input Mode	Detection Method		
	swept frequency	slew scan	multiplex
Single frequency modulation	1	—	—
multi-frequency modulation	$6.25 \times 10^{-4}$	$9.8 \times 10^{-3}$	$6.25 \times 10^{-2}$
broadband modulation	$10^{-13}$	—	$10^{-11}$

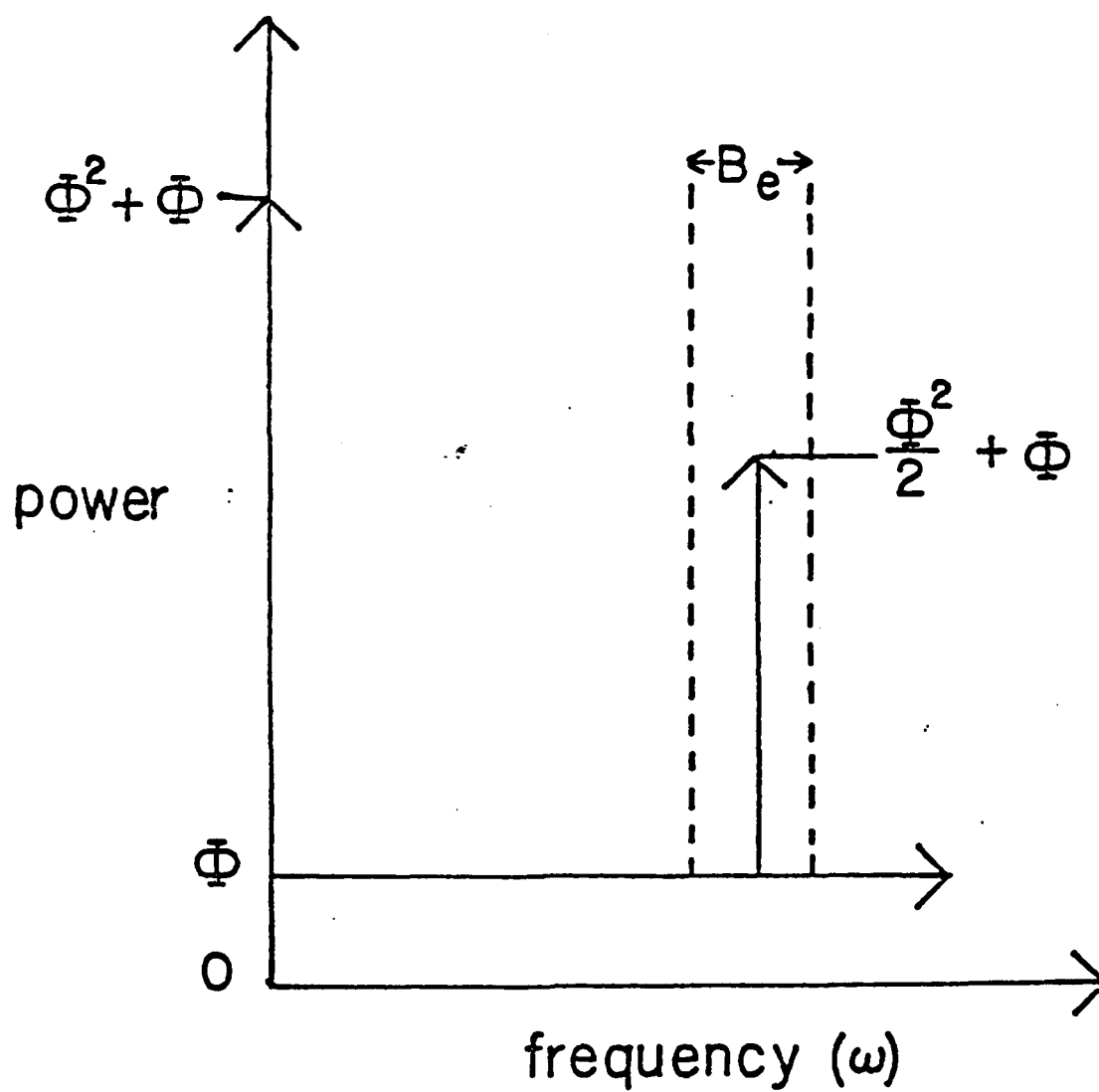
<sup>a</sup>  $B$  is the total bandwidth over which the experiment is performed,  
 $B_w$  is the detection system bandwidth, and  $K$  is the number of  
 modulation frequencies for multi-frequency modulation.

## FIGURE LEGENDS

Figure 1. Two methods for the determination of fluorescence lifetimes by frequency-response measurement. C is the fluorescence sample cell, PMT is a photomultiplier tube, and AC→DC is a device which yields a DC signal proportional to the mean square amplitude of the AC input. A. Swept single-frequency method. B. Wideband modulation method.

Figure 2. The total power spectrum (noise + signal) for the swept single-frequency method. The photon flux is 100% modulated at  $\omega_0$  and has an average value of  $\Phi$ . The bandwidth of the detection system used to measure the power at  $\omega_0$  is  $B_e$ .





TECHNICAL REPORT DISTRIBUTION LIST, GEN

	<u>No. Copies</u>		<u>No. Copies</u>
Office of Naval Research Attn: Code 413 800 North Quincy Street Arlington, Virginia 22217	2	Naval Ocean Systems Center Attn: Mr. Joe McCartney San Diego, California 92152	1
ONR Pasadena Detachment Attn: Dr. R. J. Marcus 1030 East Green Street Pasadena, California 91106	1	Naval Weapons Center Attn: Dr. A. B. Amster, Chemistry Division China Lake, California 93555	1
Commander, Naval Air Systems Command Attn: Code 310C (H. Rosenwasser) Department of the Navy Washington, D.C. 20360	1	Naval Civil Engineering Laboratory Attn: Dr. R. W. Drisko Port Hueneme, California 93401	1
Defense Technical Information Center Building 5, Cameron Station Alexandria, Virginia 22314	12	Dean William Tolles Naval Postgraduate School Monterey, California 93940	1
Dr. Fred Saalfeld Chemistry Division, Code 6100 Naval Research Laboratory Washington, D.C. 20375	1	Scientific Advisor Commandant of the Marine Corps (Code RD-1) Washington, D.C. 20380	1
U.S. Army Research Office Attn: CRD-AA-IP P. O. Box 12211 Research Triangle Park, N.C. 27709	1	Naval Ship Research and Development Center Attn: Dr. G. Bosmajian, Applied Chemistry Division Annapolis, Maryland 21401	1
Mr. Vincent Schaper DTNSRDC Code 2803 Annapolis, Maryland 21402	1	Mr. John Boyle Materials Branch Naval Ship Engineering Center Philadelphia, Pennsylvania 19112	1
Naval Ocean Systems Center Attn: Dr. S. Yamamoto Marine Sciences Division San Diego, California 91232	1	Mr. A. M. Anzalone Administrative Librarian PLASTEC/ARRADCOM Bldg 3401 Dover, New Jersey 07801	1



TECHNICAL REPORT DISTRIBUTION LIST, 051C

	<u>No. Copies</u>		<u>No. Copies</u>
Dr. M. B. Denton Department of Chemistry University of Arizona Tucson, Arizona 85721	1	Dr. L. Jarvis Code 6100 Naval Research Laboratory Washington, D.C. 20375	1
Dr. R. A. Osteryoung Department of Chemistry State University of New York at Buffalo Buffalo, New York 14214	1	Dr. John Duffin, Code 62 Dn United States Naval Postgraduate School Monterey, California 93940	1
Dr. J. Osteryoung Department of Chemistry State University of New York Buffalo, New York 14214	1	<del>Dr. G. M. Hieftje Department of Chemistry Indiana University Bloomington, Indiana 47401</del>	1
Dr. B. R. Kowalski Department of Chemistry University of Washington Seattle, Washington 98105	1	Dr. Victor L. Rehn Naval Weapons Center Code 3813 China Lake, California 93555	1
Dr. S. P. Perrone Department of Chemistry Purdue University Lafayette, Indiana 47907	1	Dr. Christie G. Enke Michigan State University Department of Chemistry East Lansing, Michigan 48824	1
Dr. D. L. Venezky Naval Research Laboratory Code 6130 Washington, D.C. 20375	1	Dr. Kent Eisentraut, MBT Air Force Materials Laboratory Wright-Patterson AFB, Ohio 45433	1
Dr. H. Freiser Department of Chemistry University of Arizona Tucson, Arizona 85721		Walter G. Cox, Code 3632 Naval Underwater Systems Center Building 148 Newport, Rhode Island 02840	1
Dr. H. Chernoff Department of Mathematics Massachusetts Institute of Technology Cambridge, Massachusetts 02139	1	Professor Isiah M. Warner Department of Chemistry Emory University Atlanta, Georgia 30322	
Dr. A. Zirino Naval Undersea Center San Diego, California 92132	1	Professor George H. Morrison Department of Chemistry Cornell University Ithaca, New York 14853	1

TECHNICAL REPORT DISTRIBUTION LIST, 051C

	<u>No. Copies</u>	<u>No. Copies</u>
Professor J. Janata Department of Bioengineering University of Utah Salt Lake City, Utah 84112	1	
Dr. Carl Heller Naval Weapons Center China Lake, California 93555	1	
Dr. Denton Elliott AFOSR/NC Bolling AFB Washington, D.C. 20362		
Dr. J. Decorpo NAVSEA-05R14 Washington, D.C. 20362		
Dr. B. E. Spielvogel Inorganic and Analytical Branch P. O. Box 12211 Research Triangle Park, NC 27709		
Dr. Charles Anderson Analytical Chemistry Division Athens Environmental Lab. College Station Road Athens, Georgia 30613		
Dr. Samuel P. Perone L-326 LLNL Box 808 Livermore, California 94550		
Dr. B. E. Douda Chemical Sciences Branch Code 4052 Naval Weapons Support Center Crane, Indiana 47522		
Ms. Ann De Witt Material Science Department 160 Fieldcrest Avenue Raritan Center Edison, New Jersey 08818		

**END**

**FILMED**

**2-83**

**DTIC**